Inferring causal connectivity from pairwise recordings enabled by optogenetics

Mikkel Elle Lepperød, Konrad Paul Kording

May 3, 2018

Abstract

Neurons interact by way of action potentials and understanding how neurons causally affect one another has been a key focus of neuroscience for decades. Measuring the activity of a fraction of the population and probe part of these, recently using optogenetics, typically leads to stimulation effects on multiple cells. This produces a confounding problem meaning that one cannot infer which of the stimulated neurons affected the activity of a putative post-synaptic neuron. Here we show how the resulting biases can be large using common methods such as cross correlation histograms (CCH) or regression analysis. We propose that using causal inference techniques, in particular instrumental variables from econometrics, can ameliorate this confounding problem. Instrumental variables allow us to better predict causal relationships between neurons from pairwise recordings with optogenetic perturbations. In our suggested approach, we utilize neurons' absolute refractory states where stimulation will not induce a new action potential. This failed response to stimulation allows disentangling causality. In simulated data sets of integrate and fire neurons receiving simulated optogenetic stimulation we show that the instrumental variable technique predict neural interactions better compared to CCH and logistic regression. Proposed instrumental variable technique falsely attributes connectivity only 0.2% compared with CCH at 13.3%. Our approach is robust and easy to implement under carefully designed experimental paradigms. To improve accuracy of causal interpretations, new experimental designs are foreseen. In experiments where random stimulation of individual neurons is impossible, causal inference techniques are necessary to identify connectivity.

1

1 Introduction

Neuroscience aims to understand the mechanisms or causal chains that give rise to activity in the brain, to perception, complex behaviors and cognition. For this, correlations between variables are insufficient to reveal or predict underlying causality. After all, there can be many ways how the same activities come about by distinct causal chains [Drton et al., 2011, Peters et al., 2017]. Identifiability of causal networks is complicated when it comes to brain data. Complex systems such as the brain are hard to understand because of the numerous ways the contributing elements may interact internally [Jonas and Kording, 2017]. Thus, brain data which is almost always observational, will almost never satisfy the criteria needed for identifiability[Pearl, 2009]. While observing correlations within the system is usually relatively easy, transitioning from observed correlations to a causal or mechanistic understanding is hard or, more common, impossible. Getting at such an understanding in the human brain is nearly impossible as it contains approximately 86 billion neurons [?], each of which influences many other neurons. Only under certain assumptions about nonlinearity or noise sources does a fully observed system become identifiable [Daniusis et al., 2012, Shimizu et al., 2006]. Even if we could record all neurons at the same time, estimating causality and producing a mechanistic understanding would be extremely challenging.

In recordings from neuroscience, we generally only record from a small subset of all neurons. The data from typical recordings, e.g. from electrophysiology or calcium imaging, is very low dimensional relative to that of the brain. Moreover, the data is observational and does not result from randomized perturbations. In such cases, it is impossible to know to what extent the observed activity was caused by other observed activity or by the activity of the unobserved neurons. Unobserved activity is called confounders. If mechanisms are estimated from observational data in the presence of condounders, we will generally make large errors and draw incorrect conclusions[Angrist and Pischke, 2008]. Unobserved neural activity confounds estimates of causal interactions and makes it difficult to estimate underlying mechanisms.

confounding is the big threat to causal validity [?] irrespective of the use of simple regression techniques or advanced functional connectivity techniques[Stevenson et al., 2008a, Honey et al., 2009]. A much used method for estimating the output of single neurons is to perform multiple regression analyses [Pillow et al., 2008], modeling each neuron with a generalized linear model (GLM). Multiple regression may be perceived as a solution

to confounding problems as they support the concept of "explaining away" [Stevenson et al., 2008a]. However, in current work we will exclude approaches that look at multiple neurons at the same time. This is because, "explaining away" can only be a good strategy if most neurons are included in the recordings but this is rarely the case for most experimental settings, especially in the mammalian brain. We will therefore focus on neuron pairs where stimulus and the pre- and post-synaptic neurons are known.

To estimate connectivity it is first and foremost important that it stems from cause and effect e.g. B's action potential is causing an increase in C's membrane potential, therefore we use the term causal connectivity. For a given example we want to estimate causal connectivity between two neurons, A and C (Fig. 2(a)). Two neurons, A and B, are driven by a common input D and because B and C are connected they are strongly correlated. Consequently, A and C are also correlated and a regression $C = \beta A$ will misleadingly conclude that there is a direct interaction if it was causally interpreted. In this case we say the regressor A is endogenous and the regression coefficient β estimates the magnitude of association rather than the magnitude of causation. Naive regressions in partially observed systems will generally not reveal causality.

To estimate causal relationships between neurons, stimulating the pre-synaptic neuron is the gold standard. In fact, a common definition of causality is in terms of what would happen if one would change the value of one variable in the system, independently of changing other variables – an intervention [Pearl, 2009]. If we stimulate single neurons, the ability to estimate causal relationships by regression is within reach. However, this is experimentally challenging and with low cell count because it either requires intracellular, juxtacellular or two-photon stimulation [?, Lerman et al., 2017, Nikolenko et al., 2007, Emiliani et al., 2015]. Because gold-standard perturbations are challenging, it would be highly desirable if causality could be obtained from optogenetic stimulation [Boyden et al., 2005, Zemelman et al., 2002].

Interpreting the results of optogenetic stimulation in terms of causal interactions is difficult. The expression of opsins are usually restricted to a population of neurons but regular optogenetic stimulation will still affect many neurons simultaneously. In *in vivo* settings it is generally impossible to direct photons to only one neuron. Hence, the stimulus will produce a distributed pattern of activity. For example, if we focus a stimulation beam on one neuron, there will be a cone of light in front of and behind the neuron. This distributed pattern of stimulation produces activity which then percolates through the network of neurons. Thus any post-synaptic

activity induced by stimulation could in principle come from any of the stimulated neurons introducing problematic confounders.

The inference of causality from observational data is addressed in the fields of statistics [Pearl, 2009], machine learning [Peters et al., 2017] and econometrics [Angrist and Pischke, 2008]. Within these fields, the problem of endogenous regressors is commonly addressed. Taking advantage from their experiences we propose to meet and solve the confounding problem induced by optogenetic stimulation to identify connectivity between neurons.

A commonly used approach towards causal inference in economics is instrumental variables. Let's say that we want to estimate the return β from education x to yearly income y with the regression $y = \beta x + u$. Here u are the factors other than education that contributes to yearly income. One of the factors in u is a person's cognitive ability. However, a person's cognitive ability may also affect education and thus the regressor x is correlated with the error term u. This will imply that the regression estimate β will not estimate the magnitude of causation from education on income, but rather, its association. In this case one may use the proximity to a college or university as an instrumental variable (IV) [Card, 1993]. Proximity is a good instrument since it can only affect income through schooling, since we expect living in proximity of colleges and universities give higher probability to attend but not to affect other contributing factors to income such as cognitive ability. Then, in order to attribute the causal effect of education on income one may calculate the ratio of covariances $\beta = cov(\text{proximity}, \text{income})/cov(\text{proximity}, \text{education})$. This ratio corrects for the confounding factor.

The IV technique has been used extensively in econometrics and is provable causal given three assumptions [Angrist and Pischke, 2008]. First, the instrument must be uncorrelated with the error term. Second, the instrument must be correlated with the regressor. Third, there must be no direct influence of the instrument on the outcome variable but only an influence through the regressor variable. The validity of these assumptions is central when using the IV.

For an instrument to be good, it needs to be unaffected by other variables. In the brain, almost everything is affected by the network state. However, certain variables can be more or less affected. For example, the overall activity of the network is through slow and strongly nonrandom dynamics. In contrast, the temporal pattern of when a neuron is in a refractory state may be random. First, if neurons are spiking according to conditional Poisson distributions, their exact timing will, conditioned on the network state, be random. Moreover, after a strong and long lasting stimulation the phases

4

of integrate and fire neurons will effectively be random. While refractoriness may not be perfectly random, the exact times of spiking are notoriously difficult to predict [Stevenson et al., 2008a] suggesting that refractoriness are likely quite random.

Here we show that the instrumental variable (IV) technique can be, and perhaps should be, employed to estimate the causal connectivity between neuron pairs. We begin by showing how confounding factors are introduced by regular optogenetic stimulations. We then simulate this confounding effect in a simple network of three leaky integrate and fire (LIF) neurons. With this simple model we show that by using the refractory period as an IV we are able to distinguish between connected and unconnected neuron pairs. We compare these estimates with a naive although widely used cross-correlation histogram (CCH) method that fails to distinguish respective pairs. We then turn to a simulated network of randomly recurrent connections of excitatory and inhibitory LIF neurons with distributed synaptic weights. With this data at hand we first calculate the mean squared errors of the IV method and show that it is robust to different simulated network states. Finally, we compare the amount and size of false positive and false negative estimates and goodness of fit on synaptic weights with pairwise assessments using CCH and logistic regression.

2 Results

2.1 Optogenetics is not local

Optogenetics is generally seen as a perturbation method that by and large affects neurons in close proximity of the light source. However, it can be questioned if this is the correct way of conceptualizing the spatial effect of stimulation. The stimulation effects depend on multiple factors. Firstly, light intensity and opsin density are important as more light and ion channels will cause a stronger effect on each cell. Secondly, the number of potentially stimulated neurons is critical as more neurons will have a larger impact on the overall population activity. Lastly, physiological properties of the cells are important as light may e.g. only have a strong effect on spiking activity when the membrane potential of the cell is sufficiently close to the firing threshold. The induced effect of optogenetic stimulation as a function of distance should be the product of four parameters: light intensity, spatial distribution of neurons, distributions of membrane potential across neurons, and opsin distribution across neurons.

To estimate the light intensity we calculated the spatial extent of laser

light delivered by fiber-optics under plausible experimental conditions according to [Aravanis et al., 2007]; see Section 4.5. This modeling of light intensity yield an approximately $1/r^2$ reduction with distance r from the light source Fig. 1 (cyan line). This is explained by the surface of the 3d shell growing with $4\pi r^2$ and photons will be roughly isotropic beyond the scattering length Fig. 1 (inset). The same number of photons has to cross each of the spheres around the stimulation location unless they are absorbed. The density of photons decreases rapidly with distance.

To estimate the density of neurons at a given distance there will be more neurons the further away they are from the stimulation site given that neurons are uniformly distributed in brain tissue Fig. 1 (black line). In fact, the number of neurons will increase by approximately r^2 with distance. This derives from the same surface scaling as for the 3D shell. Thus the number of neurons that can be activated increases rapidly with distance.

To estimate the effect of stimulation, the functionality underlying spiking activity needs to be considered. This can largely be characterized by the distribution of membrane potentials across neurons. Surprisingly, this distribution has been observed to be symmetrically distributed [Paré et al., 1998, ?, ?, Rudolph and Destexhe, 2006]. This suggest that the response in membrane potential to a perturbation for any neuron is roughly proportional to the light intensity. Moreover, assuming that opsins are evenly distributed along the neuron, the opsin density in the neuron population will be relatively even. Based on this, we calculate the overall stimulation effect to be the product of neuron density and light intensity which is approximately constant in distance (up to the distance where absorption becomes important) Fig. 1 (blue line). Thus, optogenetic stimulation utilizing single photon activation does not actually produce a localized effect.

2.2 Confounding as a problem for the estimation of causal effects

When we stimulate many neurons at the same time, and observe a post-synaptic neuron to be active after our stimulation, it is hard to know which of the stimulated neurons produced the activity. To illustrate such confounding effects we simulated a network comprised of three neurons (A,B, and C). The neurons receive Poisson spike trains and have added Gaussian white noise to the membrane potential. We also gave them interactions, where spikes of neuron B increase the probability of firing for neuron C but there are no other interactions Fig. 2(a). Finally, we allowed simulated optogenetic stimulation to affect neurons A and B (but not C). We thus have a simple
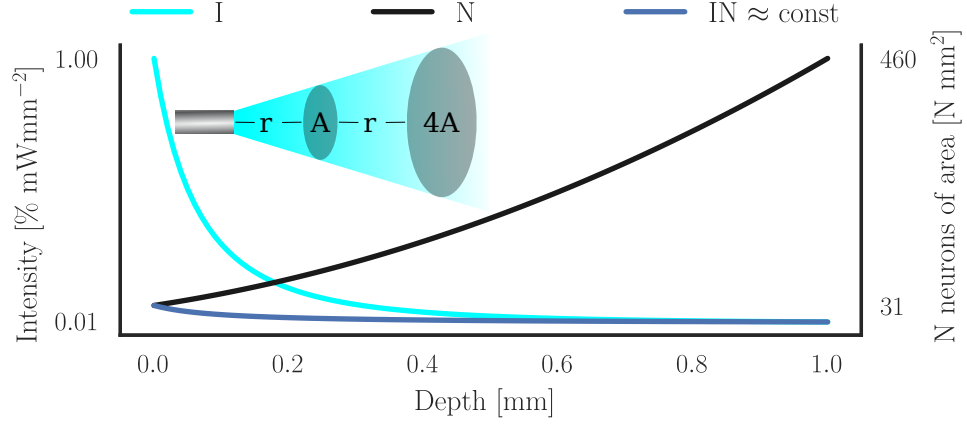
Figure 1: **Spatial extent of optogenetic stimulus**. Due to scattering and geometric loss the light intensity (I, cyan line) plotted as percentage of intensity exiting the optogenetic fiber follows approximately an inverse square law r^{-2} where r is the distance from the fiber. If neurons are uniformly distributed the number of affected neurons increase by r^2 (N, black line) rendering the probability of activating a neuron approximately constant (IN, blue line).

system for exploring questions of causality.

After running the simulation, the peri-stimulus time histogram of the stimulated neurons show the result of both the stimulation itself (suppressed for visibility) and the neuron's refractory period Fig. 2(b) (AA, BB). Since the stimulation affects A and B simultaneously, it induces a strong correlation between A and B Fig. 2(c) (AB). This further generates a strong correlation between A and C, confounding the system by rendering the cross correlation histograms (CCHs) between BC and AC both statistically significant ($p_{\text{fast}} < 0.001, p_{\text{diff}} < 0.001$; see Section 4.2) shown in Fig. 2(c). Even though the correlation peak between B and C is larger than between A and C due to correlated spikes outside the periods with stimulation one may imagine a situation where only A and C is measured, giving rise to a false prediction that they are connected. If stimulation affects multiple neurons simultaneously, there is a real confounding problem.

2.3   Instrumental variables to resolve confounding

If we want to discover the actual influence of stimulation of a neuron on post-synaptic neurons we need something that can distinguish the influence from one stimulated neuron from the influence of another stimulated neuron. We would thus need something that affects the stimulation effect on only one neuron. Arguably, refractoriness is such a variable. If a neuron is in its absolute refractory period, then no amount of stimulation will make it spike. This allows us an interesting way of getting at causality, by comparing the network state between a time when a neuron is able to spike and a time where the neuron is unable to spike.

Instrumental variables requires the existence of a random (or sufficiently random) variable that affects a variable of interest. This independent influence then allows quantifying the influence of the variable of interest on the rest of the network. In our case, the refractory times of a neuron is in good approximation independent on small time scales (see Discussion for caveats). It affects the influence of stimulation on the potentially pre-synaptic neuron (Fig. 3(a)). The spikes that are thus missing from the refractory neuron, which otherwise would have been induced by the stimulation, can then be used to identify causal effect on the potentially post-synaptic neuron.

We can now test if, for our simple three neuron system, use of an instrumental variable estimator would do better than simply analyzing the correlations by looking at the cross correlation histogram (CCH). We thus use the IV estimator Eq. (4) on the three neuron system (Fig. 3(b) and (c)). It converges to the correct causal conclusions that the weights $w_{BC} > 0$ and
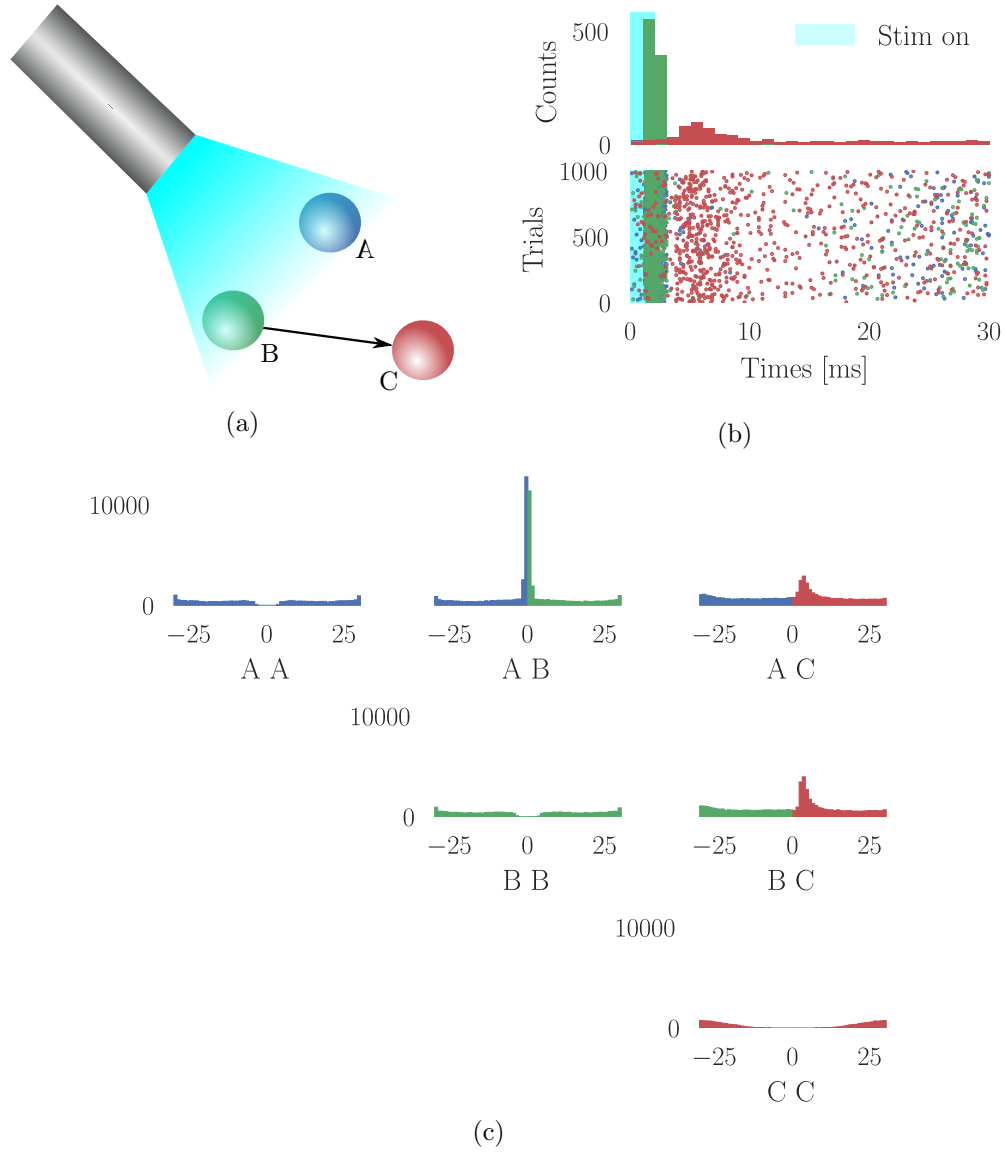
8

Figure 2: **A,B,C network**. A sketch of the simple network containing three neurons shows stimulation configuration with blue laser light and the connections with arrows (a). The neurons A and B are stimulated 1000 trials and the corresponding peristimulus time histogram are shown in (b) upper panel with a raster plot in the lower panel. Cross correlation histograms (CCHs) are shown in (c) where horizontal and vertical axes represents time lag in ms and counts of coincident spikes in bins of 1 ms.

9

$w_{AC} = 0$. For such a simple system, it produces meaningful estimates of the causal interactions between neurons.

2.4 Larger simulated networks

The interacting neurons in a biological network exhibit inhibition and interact in many kinds of ways. To evaluate the IV method in a more meaningful setting we thus simulated a recurrent neural network consisting of 1250 randomly connected leaky integrate and fire neurons where 250 had inhibitory synapses. The network was tuned to be in an asynchronous regime; see Fig. 6(a) with log-normally distributed synaptic weights according to patch clamp experiments [Sayer et al., 1990, Mason et al., 1991]; see Fig. 6(c) and Table 1 for parameters. Further, we selected 800 excitatory neurons for stimulation and gave each neuron a random spatial distance from the simulated optogenetic stimulus. The stimulus intensity was then set according to Eq. (15) with a maximum of 10 pA, and was constant throughout trials. The trial onset had a temporal Poisson distribution with period 100 ms and was further clipped between 100-150 ms. For weight estimates we randomly selected among the excitatory population 50 stimulated neurons and 50 unstimulated neurons.

To evaluate how well the IV method estimates the weights as a function of number of trials we calculated the mean squared error of the weight connecting the 100 neuron pairs Fig. 4. As seen here, the IV estimator's precision decreases similarly in three different settings with varying amounts of relative inhibition g. We want to compare the IV estimator which exploits the refractory period with the CCH method given by Eq. (6) which ignores network confounding. To indicate the amount of connections which are falsely attributed a non-zero weight we calculated the amount of false positives. This was given as the percentage of estimated synapses larger than 0.05 where the true weight was 0, finding 13.3% for CCH and 0.2% for the IV estimator; see Fig. 5(a). In addition we compared the size of the estimations at false positive instances and found that the CCH give significantly higher false positive weight-estimates than IV ($p = 0.03$ $\Delta = 0.049$, calculated by permutation re-sampling [Wassermann, 2006]; see Fig. 5(a). The IV approach, while not being perfect, thus outperforms the simple CCH approach.

It might be that modeling refractory periods in the context of a naive regression estimates connectivity equally well as the IV method. We thus performed a logistic regression as seen in Fig. 5(a) denoted logit. As seen here, logit performs even worse than CCH showing that it really helps to use
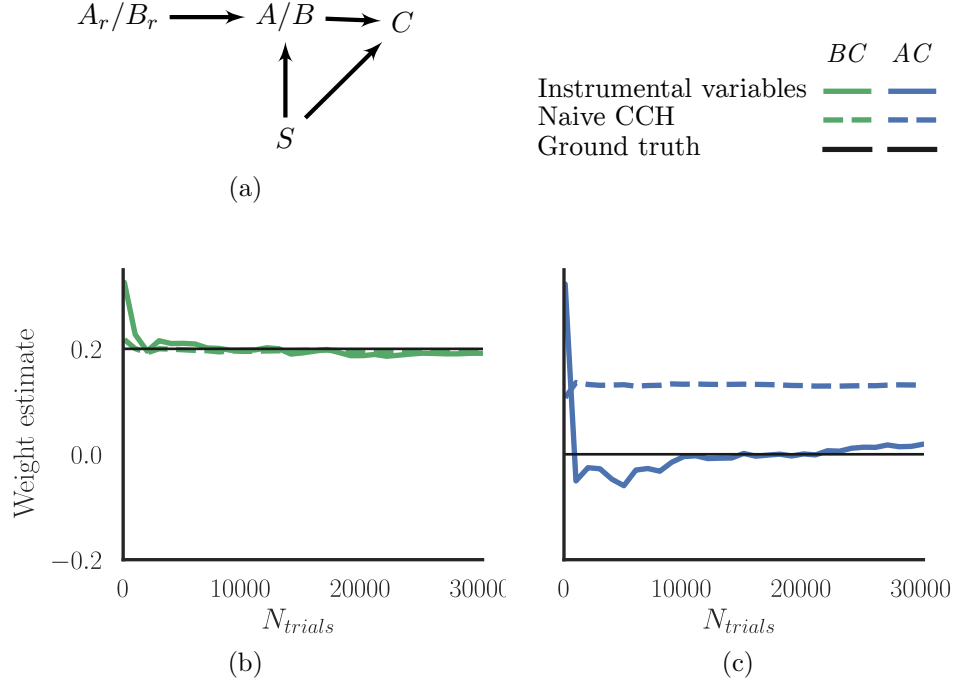
Figure 3: **Instrumental variable estimation (IV) of connectivity**. (a) In an instrumental variable estimation procedure we use a variable that is assumed to be random (here refractoriness) which influences a variable of interest (here spiking) and to use this influence to infer the causal interaction of that variable on other variables (here spiking of A or B onto C). (b) A popular estimation approach for IVs, the Wald technique correctly estimates causal connectivity in the A,B,C neural network using the refractory period. Subfigure (a) shows a path diagram [**?**] between the upstream neuron A or B, the stimulation S, the post-synaptic neuron C and the IV as A_r or B_r. Arrows represent associations where S is associated with A, B and potentially also with C both directly and through A, B. The IV estimator calculated by Eq. (4) converges to $\hat{\beta}_{BC} \approx 0.2, \hat{\beta}_{AC} \approx 0$ after approximately 5000 trials as seen in (b) and (c) respectively. Insets represent high resolution zoom of cross correlation histograms of BC and AC where horizontal and vertical axes represents time lag and counts of coincident spikes in bins of 0.1 ms respectively.
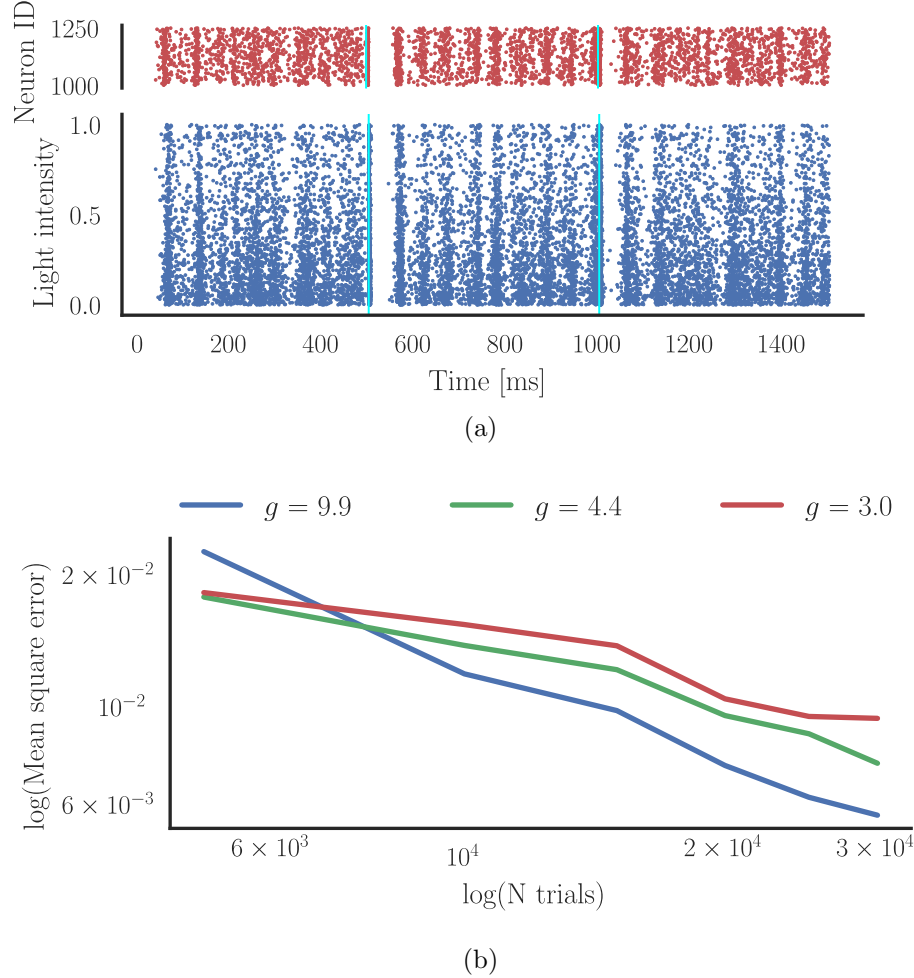
(a)

(b)

Figure 4: **Mean square error (MSE) of IV estimator in a large network**. (a) Excitatory neurons (in blue raster) are stimulated with varying intensity indicated by the y-axis in lower panel, upper panel shows inhibitory neurons (red raster) where y-axis indicate random neuron-id. (b) The IV estimator is evaluated in the asynchronous recurrent neural network at three different amounts of relative inhibition g (decreasing with model number). The MSE as a function of number of trials is shown on a logarithmic scale where the slopes was found to be $-0.77, -0.48, -0.40$ for model 1,2,3 respectively.

12

the refractory period as an instrumental variable. To further evaluate the methods we calculated false negatives as instances where the true weight is non-zero but estimated to be equal to zero in Fig. 5(b) showing that the CCH and IV estimators performs equally well. Finally we wanted to evaluate the estimated weights as a function of true weights shown in Fig. 5(c) and (d) after 30000 trials. The IV estimator yields a good prediction $r^2 = 0.55$, while the CCH estimator performs surprisingly bad with $r^2 = 0.002$. Utilizing refractory periods as an (imperfect) instrumental variable considerably improves estimates.

3 Discussion

Here we have asked if the refractory period of neurons can be used as an instrumental variable to reverse engineer the causal flow of activity in a network of simulated neurons. We have found that this approach performs considerably better than the naive method. We have found that neither naive linear nor naive logit models produce good estimates of weights. Our system effectively reverse engineers causality by looking at the response that is missing because of refractoriness which effectively allows better estimates of causal effects.

One popular way of estimating causal effects is fitting generalized linear models (GLMs) to simultaneously recorded neurons[Pillow et al., 2008]. The GLMs are basically multiple regressions and require multiple neurons in order to perform well. In fact, if one recorded all neurons, GLMs could be sufficient to estimate causal connections. However, this is not the case for research in the mammalian brain, especially not for primates, where we only record a very small subset of the neurons that do the actual computation. The GLM field is very strong at modeling latency distributions and sequences of spikes in individual neurons. These ideas should, arguably, be merged with IV approaches. The main strength of the IV estimator presented here compared with GLM methods is that we only require one pair because we can utilize the randomness in refractoriness.

The main problem with optogenetics when using it to infer connectivity is its non-local property. This is due to the inverse relation between changes in light intensity and affected number of neurons combined with the observation that distributions of membrane potentials across neurons are symmetrically distributed [**?**, Rudolph and Destexhe, 2006, Paré et al., 1998, **?**]. One could however imagine situations where optogenetic activation were more local. If membrane potential distributions were in general
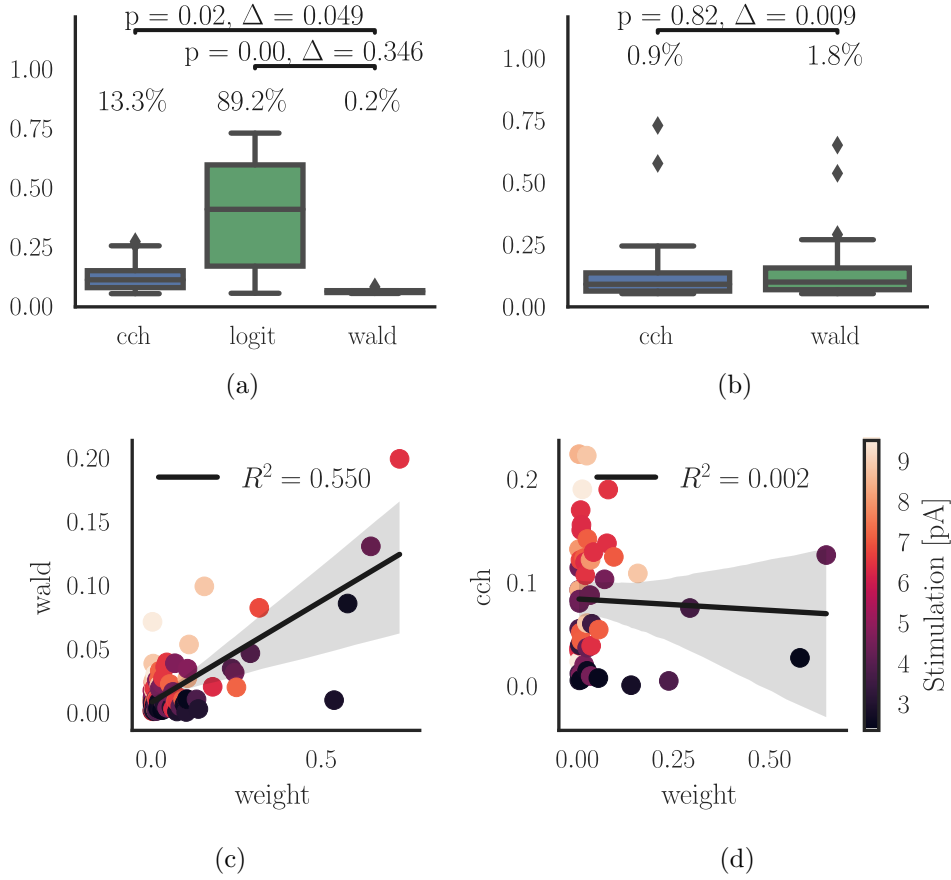
Figure 5: **False estimates and goodness of fit**. False positives are shown in (a) for the cross correlation histogram (cch) method, logistic regression (logit) and the IV estimator (wald). False negatives for cch and wald is shown in (b). Positive estimates of weight as a function of true weight is scattered for the wald estimator in (c) and cch in (d) color coded by the size of perturbation intensity.

skewed with the mode far from threshold the optogenetic perturbation would be more local. This is because each neuron would require a very strong stimulus in order to elicit spikes at all. But there could be other ways of making optogenetics more local. For example, if one could engineer opsins with far more absorbent wavelengths one could stimulate locally. How to engineer more localized stimulation is an important problem if one wants to causally interrogate systems.

Very weak laser pulses in noisy networks might only affect very few neurons each trial [English et al., 2017]. However, the stimulus will still affect the many far away neurons by a tiny bit. Therefore, weak stimulation does not remove the principal problem of the CCH estimator. Moreover, the network still acts as a confounder and, if anything, the weak stimulation will dramatically reduce the statistical power of the approach. Lowering stimulation amplitudes does not appear to be a way of obtaining meaningful causal estimates.

For the refractory period to be a good instrument, it is necessary that it is not overly affected by the network activity. This clearly is going to be problematic in many cases, after all the network activity affects refractoriness. However, there are multiple scenarios where refractoriness will be a good instrument. For example, if we have balanced excitation and inhibition we may expect largely independent refractory states of individual neurons. If a neuron biophysically implements something like conditional Poisson spiking its refractory states will be random. Even if neurons refractory states are strongly correlated during normal network operation there may be ways of randomizing them. Giving one burst of stimulation which is strong enough to elicit multiple spikes from each neuron may effectively randomize the phase of each neuron [?]. Importantly, we may expect the phase of a neuron to be far more random than the activity of the network as a whole.

We found some negative values of the IV estimator which were suppressed as we knew that we only stimulated excitatory neurons. This happens because neurons have correlated refractory times which is likely when looking at the distribution of CC seen in Fig. 6(a). Furthermore, the neural network simulated here introduces much response overlap due to synapses having equal synaptic time constants and transfer delays. This makes inference quite hard since multiple neurons are affecting the same cell at the same time for each stimulation. However, this is less important in the brain, where the variability of connections and synaptic weights and where firing patterns are sparser would most likely work to the advantage of the IV method. Independence of refractoriness would be further improved, if in

15

addition a clever stimulation routine was implemented such that the distribution of stimulation strength varies spatially from trial to trial.

The independence of refractory times is the one factor which makes or breaks the IV approach. Therefore we may think of ways of making the refractoriness distribution more random. First, it would help to use a task and situation where neurons are as uncorrelated as possible. Second, we may use a set of conditioning pulses of stimulation to increase independence of refractory states. Third, we may utilize chemical, behavioral, or molecular perturbations to randomize refractoriness. There has not, to the authors knowledge, been any attempts in neuroscience to randomize times of refractory states, so there may be a lot of possibilities to improve.

Generalizing this idea, we may ask if there are ways of constructing good instrumental variables. One may assume a way of building molecular oscillators or otherwise pattern generators into neurons which affect their firing rate. Such modulatory activity would be observable in the extracellular activity of the neuron. Any neuron that then correlates to this modulation must be post-synaptic of the recorded neuron. Any kind of a signal that is local to a cell and not affected by network activity could produce a meaningful instrumental variable and it might be reasonably doable to link membrane channels to intracellular signal generation. Even if perfect IVs do not exist in brains, we may be able to make them.

There are many techniques for causal inference and most of them are largely unknown in neuroscience and are based on approximating randomness in a world that does not have it. In many cases, one could use regression discontinuity designs if one has a spiking system [?, ?]. One could use a difference in difference approach [?]. One can use matching approaches [?], but see [?], where one compares similar network states and their evolution over time. In general, neuroscience is in a quest for causal interpretations, we should be able to benefit considerably by utilizing techniques that are popular in the field of causal inference.

4 Methods

4.1 Instrumental variable estimation

A simple approximation of the connectivity strength between a pre-synaptic neuron x and post-synaptic neuron y can be to ignore external excitation and simply calculate the relation between the spike times in x and y with a regression model given by

$$y = \beta x + u. \tag{1}$$

Here y is the dependent variable, x is the explanatory variable, β is the effect of the x on y and u is an unknown error term. This system follows the path diagram [?]
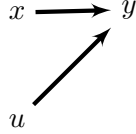
Assuming that changes in spike times y are described by βx i.e. $\frac{\mathrm{d}y}{\mathrm{d}x} = \beta$ for spike times x. One problem with this idea is that in a confounded system, perfectly correlated neurons will give statistically indistinguishable β. In the extreme case where two neurons are both made to fire every time they are stimulated, they will have the same weights according to Eq. (1). After all, during stimulation $y = 1$ for both, even if only one of them drives the post-synaptic neuron. Another problem is if the network state affects both the probability of a neuron to fire and also the probability of post-synaptic neurons to fire. In this case, the network state can induce a correlation which will make the estimation highly biased. Arguably, the network state will, in all realistic models, have a dramatic influence on all neurons and the regression model is better described by

$$y = \beta x + u(x). \tag{2}$$

Corresponding to the following path diagram
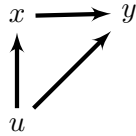
Here we have the relation $\frac{\mathrm{d}y}{\mathrm{d}x} = \beta + \frac{\mathrm{d}u}{\mathrm{d}x}$. To get at causality we thus require some stimulation that only highlight the activity in y caused by x, disassociating x from u. However, the optogenetic stimulation is not specific to x and will activate parts of the network activity u. Let us assume that the stimulus renders only a subset of u correlated with x, namely u_s. To disassociate x from u_s we need something that can distinguish between different neurons that are stimulated. We thus require some instrument x_r

which is (1) uncorrelated with the network u and (2) is correlated with the regressor x[Angrist and Pischke, 2008]. We assume that the neurons are independent at small time scales and that stimulation additionally randomize membrane potential individually in neurons. We may thus use the fact that a neuron that has fired just before the stimulation will be in an absolute refractory state and hence have $x_r = 0$ independently of u. This introduces times where the spike from one of the stimulated neurons are missing. Thus we may use the refractory period as an instrumental variable, as illustrated with the following path diagram
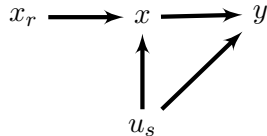
Here x_r represent times where the pre-synaptic neuron is refractory during stimulation. This is then an estimator that compares the post-synaptic activity when a given neuron is non-refractory with the post-synaptic activity when it is refractory, thus removing the confounding. The true β is given by

$$\beta_{IV} = \frac{\mathrm{d}y}{\mathrm{d}s_r} \Big/ \frac{\mathrm{d}x}{\mathrm{d}s_r} \tag{3}$$

Since our instrument x_r is binary we may use the IV (or more precisely Wald) estimator [Wald, 1940, Cameron and Trivedi, 2005] to estimate β_{IV} by

$$\hat{\beta}_{IV} = \frac{\bar{y}_s - \bar{y}_{s_r}}{\bar{x}_s - \bar{x}_{s_r}} = \bar{y}_s - \bar{y}_{s_r} \tag{4}$$

Here $\bar{y}_s$ is the average number of trials where successfully stimulating x resulted in a response in y and $\bar{y}_{s_r}$ is the average number of trials where an unsuccessful stimulation of x resulted in a response in y. The successful stimulations of x are denoted x_s and thus $\bar{x}_s \equiv 1$. Conversely x_{s_r} denotes unsuccessful stimulations of x i.e. stimulations of x during its refractory state and $\bar{x}_{s_r} \equiv 0$.

To utilize the refractory period as an IV we first picked out one window of 4 ms for each of the pre-synaptic and post-synaptic neuron with a latency relative to stimulation time of 0 and $\tau_{syn} + D$ ms (see Eq. (10)) respectively. By classifying each window for each trial whether x contained a spike we obtained the two binary arrays y_s and y_{sr}.

4.2 Cross correlation histogram

The statistical tests giving the probabilities p_{diff} and p_{fast} were done according to [Stark and Abeles, 2009, English et al., 2017]. Briefly, to test if the cross correlation histogram (CCH) peak was significant we employed two tests. By using the Poisson distribution with a continuity correction [Stark and Abeles, 2009] given by Eq. (5) we calculated p_{diff} by comparing the peak in positive time lag with the maximum peak in negative time lag [English et al., 2017]. The probability p_{fast} represents the difference between CCH and it's convolution with a hollow Gaussian kernel [Stark and Abeles, 2009].

$$p(N|\lambda(m)) = 1 - \sum_{k=0}^{N-1} \frac{e^{-\lambda(m)}\lambda(m)^k}{k!} - \frac{e^{-\lambda(m)}\lambda(m)^N}{2N!} \tag{5}$$

Here λ represents the counts at bin m and N is the number of bins considered. To estimate the connection weight between pairs we used the spike transmission probability defined in [English et al., 2017] as

$$P_{trans} = \frac{1}{n} \sum_{m=4ms}^{8ms} CCH(m) - \lambda_{Gauss}(m), \tag{6}$$

where n is the number of spikes detected in the presynaptic neuron.

4.3 Logistic regression

To utilize the refractory period without using it as an IV we estimated synaptic weights using a logistic regression. To do this we first picked out one window of 4 ms for each of the pre-synaptic and post-synaptic neuron with a latency relative to stimulation time of 0 and $\tau_{syn} + D$ ms (see Eq. (10)) respectively. By classifying each window for each trial whether it contained a spike we obtained two binary arrays, the regressor x and the dependent variable y where we want to estimate the probability $P(y = 1|x)$ by fitting the parameters $\boldsymbol{\beta}$ such that

$$y = \begin{cases} 1 & \text{if } \beta_0 + \beta_1 x + u > 0 \\ 0 & \text{else} \end{cases} \tag{7}$$

where u is an error term. Further, we used the logit link function such that the the probability giving the proxy for synaptic weight is given by

$$p(x) = \frac{1}{1 + e^{-(\beta_0 + \beta_1 x)}} \tag{8}$$

The model was fitted using the python package scikit-learn [Pedregosa et al., 2011]

4.4 Simulated network

To simulate a recurrent network of excitatory and inhibitory neurons we used the leaky integrate and fire (LIF) model given by

$$\frac{\mathrm{d}V_m^i}{\mathrm{d}t} = -\frac{(V_m^i - E_L)}{\tau_m} + \frac{I_{syn}^i(t)}{C_m}. \tag{9}$$

When the membrane potential V_m^i of neuron i reaches a threshold V_{th} an action potential is emitted and V_m^i reset to the leak potential E_L followed by an absolute refractory period τ_{ref}. The membrane time constant is represented by τ_m and $I_{syn}^i(t)$ denotes the post synaptic current (PSC) for neuron i modeled as a sum of alpha functions given by

$$I_{syn}^i(t) = \sum_{j=1}^{C} J_j \alpha(t - t_j - D), \tag{10}$$

where t_j denotes an incoming spike through synapse j at delay D and C is the number of incoming synapses on neuron i. The PSC amplitude is given by J_j and the alpha function is given by

$$\tau_{syn}\alpha(t) = te^{-\frac{t}{\tau_{syn}}}H(t). \tag{11}$$

Here τ_{syn} denotes the synaptic integration time constant and H is the Heaviside step function. All neurons were driven by an external Poisson process with rate $rate_p$.

Synaptic weights were log-normally distributed such that the increase in membrane potential V_m^i due to one spike were restricted to lie between $V_{syn} = 0.05mV$ and $V_{syn} = 2.05mV$ based on experimental findings [Sayer et al., 1990, Mason et al., 1991]. The synaptic distribution is shown in Fig. 6(c) where the inhibitory PSC amplitude is given by $J_{in} = gJ_{ex}$ where J_{ex} denotes the excitatory synaptic weight.

To find suitable parameters yielding asynchronous activity we measured the population correlation coefficient given by

$$\langle CC \rangle_{pop} = \left\langle \left\langle \frac{h_i - \langle h_i \rangle}{std(h_i)} \frac{h_j - \langle h_j \rangle}{std(h_j)} \right\rangle \right\rangle_{pop}, \tag{12}$$

where h is the spike time histogram with binsize at $5ms$ for neuron i,j and $\langle \cdot \rangle$ is the mean operator. The distribution of CC is shown in Fig. 3 which were found by performing several parameter sweeps picking three parameter sets which mainly differed in firing rate (data not shown).

To further evaluate the network state we calculated the coefficient of variation (CV) of the population given by

$$\langle CV \rangle = \left\langle \frac{std(ISI_i)}{\langle ISI_i \rangle} \right\rangle_{pop}, \tag{13}$$

where ISI denotes the inter-spike interval of neuron i. Due to the finite time synaptic integration time constant $\tau_{syn} = 1ms$ we were unable to have the network showing an irregular state; see Fig. 6(b). To verify that indeed this was due to τ_{syn} we performed several simulations with lower τ_{syn} obtaining $\langle CV \rangle_{pop} > 1$ (data not shown). It would likely be easier to achieve irregular network state if synapses were conductance based [Kumar et al., 2008]. However, we settled with current based synapses as we were mainly interested in achieving an asynchronized state ($\langle CC \rangle_{pop} < 0.01$).

4.5 Perturbation intensity

In order to replicate an optogenetic experiment we modeled transmission of light through brain tissue with the Kubelka-Munk model for diffuse scattering in planar, homogeneous, ideal diffusing media given by

$$T = \frac{1}{Sz + 1}. \tag{14}$$

Here T denotes a transmisison fraction, S is the scattering coefficient for mice [Aravanis et al., 2007] and z is the distance from a light source [Ho et al., 2017]. Further we combined diffusion with geometric loss assuming that absorption is negligible as in [Aravanis et al., 2007] and computed the intensity as presented in Fig. 1 by

$$\frac{I(r)}{I(r = 0)} = \frac{\rho^2}{(Sr + 1)(r + \rho)^2} \tag{15}$$

where r is the distance from the optical fiber and

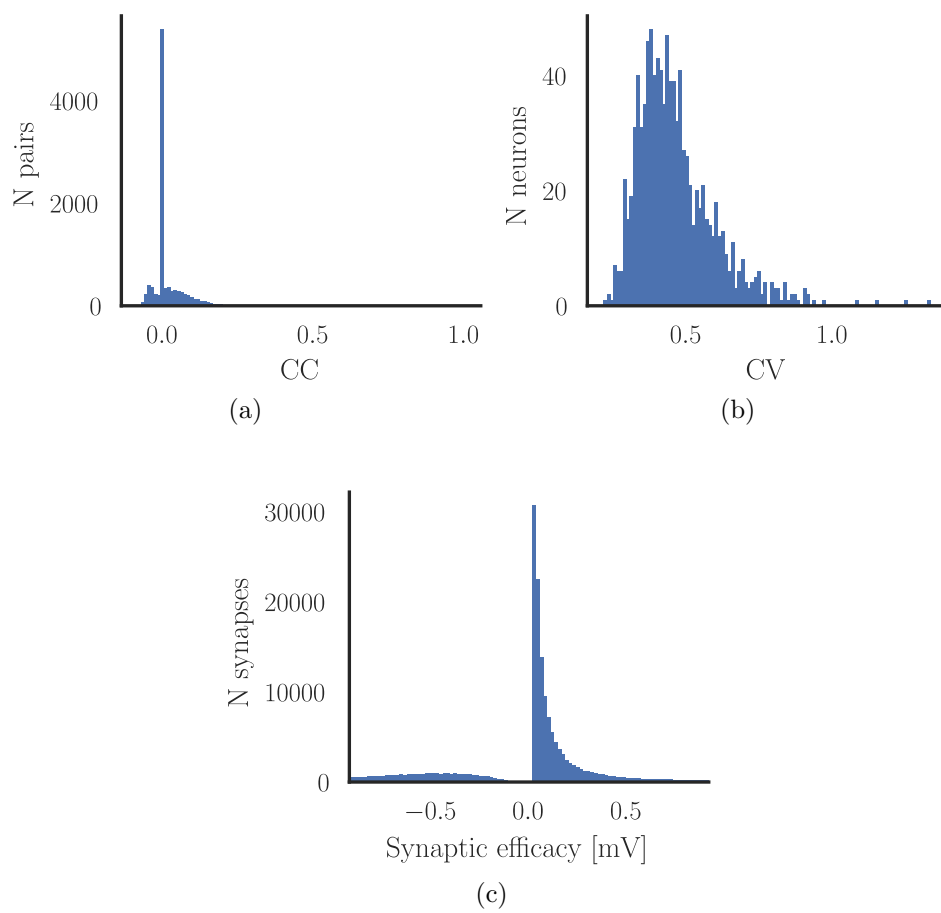$$\rho = \frac{d}{2}\sqrt{\left(\frac{n}{NA}\right)^2 - 1}. \tag{16}$$

(a)

(b)

(c)

Figure 6: Network state

	model 1	model 2	model 3	units
$N_{neurons}$	1250			
Δt	0.1			
N_{ex}	1000			
N_{in}	250			
eta	0.9			
$rate_p$	3694.26			Hz
V_{reset}	0			mV
V_m	0			mV
E_L	0			mV
t_{ref}	2			ms
τ_m	20			ms
V_{th}	20			mV
C_m	1			pF
V_{syn}	0.2			mV
g	9.9	4.4	3	
V_{syn}^{high}	2.05			mV
V_{syn}^{low}	0.05			mV
var_{syn}	0.5			mV^2
τ_{syn}^{in}	1			ms
τ_{syn}^{ex}	1			ms
$delay$	1.5			ms
eps	0.1			
C_{ex}	100			
C_{in}	25			
J_{in}	0.88727	0.394342	0.26887	pA
J_{ex}	0.0896232			pA
J_{high}^{ex}	0.918638			pA
J_{low}^{ex}	0.0224058			pA
J_{high}^{in}	0.918638			pA
J_{low}^{in}	0.0224058			pA
$stim_N^{in}$	0			
$stim_N^{ex}$	800			
$stim_{amp}^{in}$	0			pA
$stim_{amp}^{ex}$	10			pA
$stim_{duration}$	2			ms
$stim_{period}$	100			ms
$stim_{max}^{period}$	150			ms
$rate_{in}$	7.17024	9.66335	11.754	Hz
$rate_{ex}$	9.05793	10.9176	13.1032	Hz
$density$	100000			Nmm^{-3}
S	10.3			mm^{-1}
NA	0.37			
r	0.1			μm
n	1.36			

Table 1: Simulation parameters of three different models.

Here d is the diameter of the optical fiber, NA is the numerical aperture of the optical fiber and n is the refraction index for gray matter [Ho et al., 2017]; see numerical values for parameters in Table 1.

To estimate the distribution of light intensity on affected neurons we assumed a neuron density of $10^4 Nmm^{-3}$ and found the volume of a cut cone that could contain the number of stimulated excitatory neurons which were found to yield the depth $r_{max} = 0.175mm$. We then selected $N_s tim$ neurons that were given a random position in the range $[0, r_{max}]$ and were assigned a stimulation strength as the maximum stimulation strength multiplied by Eq. (15). Then we selected 50 of the excitatory neurons that were not stimulated as the "target" population which together with the inhibitory neurons were not perturbed directly by the light stimulus.

In order to keep the stimulus model as simple as possible we let set the maximum stimulation strength to $10pA$ which was found suitable by investigating the percentage of successful stimulations to be around 50%.

References

[Angrist and Pischke, 2008] Angrist, J. D. and Pischke, J.-S. (2008). *Mostly harmless econometrics: An empiricist's companion*. Princeton university press.

[Aravanis et al., 2007] Aravanis, A. M., Wang, L. P., Zhang, F., Meltzer, L. A., Mogri, M. Z., Schneider, M. B., and Deisseroth, K. (2007). An optical neural interface: in vivo control of rodent motor cortex with integrated fiberoptic and optogenetic technology. *J. Neural Eng.*, 4(3):S143–S156.

[Boyden et al., 2005] Boyden, E. S., Zhang, F., Bamberg, E., Nagel, G., and Deisseroth, K. (2005). Millisecond-timescale, genetically targeted optical control of neural activity. *Nature neuroscience*, 8(9):1263.

[Cameron and Trivedi, 2005] Cameron, A. C. and Trivedi, P. K. (2005). *Microeconometrics: methods and applications*. Cambridge university press.

[Card, 1993] Card, D. (1993). Using geographic variation in college proximity to estimate the return to schooling. Technical report, National Bureau of Economic Research.

[Daniusis et al., 2012] Daniusis, P., Janzing, D., Mooij, J., Zscheischler, J., Steudel, B., Zhang, K., and Schölkopf, B. (2012). Inferring deterministic causal relations. *arXiv preprint arXiv:1203.3475*.

[Drton et al., 2011] Drton, M., Foygel, R., and Sullivant, S. (2011). Global identifiability of linear structural equation models. *The Annals of Statistics*, pages 865–886.

[Emiliani et al., 2015] Emiliani, V., Cohen, A. E., Deisseroth, K., and Häusser, M. (2015). All-optical interrogation of neural circuits. *Journal of Neuroscience*, 35(41):13917–13926.

[English et al., 2017] English, D. F., McKenzie, S., Evans, T., Kim, K., Yoon, E., and Buzsáki, G. (2017). Pyramidal Cell-Interneuron Circuit Architecture and Dynamics in Hippocampal Networks. *Neuron*, 96(2):505–520.

[Ho et al., 2017] Ho, A. H. P., Kim, D., and Somekh, M. G. (2017). *Handbook of photonics for biomedical engineering.*

[Honey et al., 2009] Honey, C., Sporns, O., Cammoun, L., Gigandet, X., Thiran, J.-P., Meuli, R., and Hagmann, P. (2009). Predicting human resting-state functional connectivity from structural connectivity. *Proceedings of the National Academy of Sciences*, 106(6):2035–2040.

[Jonas and Kording, 2017] Jonas, E. and Kording, K. P. (2017). Could a Neuroscientist Understand a Microprocessor? *PLoS Comput. Biol.*, 13(1):1–24.

[Kumar et al., 2008] Kumar, A., Schrader, S., Aertsen, A., and Rotter, S. (2008). The high-conductance state of cortical networks. *Neural Comput.*, 20(1):1–43.

[Lerman et al., 2017] Lerman, G. M., Gill, J. V., Rinberg, D., and Shoham, S. (2017). Two photon holographic stimulation system for cellular-resolution interrogation of olfactory coding. In *Optics and the Brain*, pages BrM3B–5. Optical Society of America.

[Mason et al., 1991] Mason, a., Nicoll, A., and Stratford, K. (1991). Synaptic transmission between individual pyramidal neurons of the rat visual cortex in vitro. *J. Neurosci.*, 11(January):72–84.

[Nikolenko et al., 2007] Nikolenko, V., Poskanzer, K. E., and Yuste, R. (2007). Two-photon photostimulation and imaging of neural circuits. *Nature methods*, 4(11):943.

[Paré et al., 1998] Paré, D., Shink, E., Gaudreau, H., Destexhe, A., and Lang, E. J. (1998). Impact of spontaneous synaptic activity on the resting properties of cat neocortical pyramidal neurons in vivo. *Journal of neurophysiology*, 79(3):1450–1460.

[Pearl, 2009] Pearl, J. (2009). *Causality.* Cambridge university press.

[Pedregosa et al., 2011] Pedregosa, F., Varoquaux, G., Gramfort, A., Michel, V., Thirion, B., Grisel, O., Blondel, M., Prettenhofer, P., Weiss, R., Dubourg, V., Vanderplas, J., Passos, A., Cournapeau, D., Brucher, M., Perrot, M., and Duchesnay, E. (2011). Scikit-learn: Machine learning in Python. *Journal of Machine Learning Research*, 12:2825–2830.

[Peters et al., 2017] Peters, J., Janzing, D., and Schölkopf, B. (2017). *Elements of causal inference: foundations and learning algorithms.* MIT Press.

[Pillow et al., 2008] Pillow, J. W., Shlens, J., Paninski, L., Sher, A., Litke, A. M., Chichilnisky, E., and Simoncelli, E. P. (2008). Spatio-temporal correlations and visual signalling in a complete neuronal population. *Nature*, 454(7207):995.

[Rudolph and Destexhe, 2006] Rudolph, M. and Destexhe, A. (2006). On the use of analytical expressions for the voltage distribution to analyze intracellular recordings. *Neural computation*, 18(12):2917–2922.

[Sayer et al., 1990] Sayer, R. J., Friedlander, M. J., and Redman, S. J. (1990). The time course and amplitude of EPSPs evoked at synapses between pairs of CA3/CA1 neurons in the hippocampal slice. *J. Neurosci.*, 10(3):826–836.

[Shimizu et al., 2006] Shimizu, S., Hoyer, P. O., Hyvärinen, A., and Kerminen, A. (2006). A linear non-gaussian acyclic model for causal discovery. *Journal of Machine Learning Research*, 7(Oct):2003–2030.

[Stark and Abeles, 2009] Stark, E. and Abeles, M. (2009). Unbiased estimation of precise temporal correlations between spike trains. *J. Neurosci. Methods*, 179:90–100.

[Stevenson et al., 2008a] Stevenson, I. H., Rebesco, J. M., Miller, L. E., and Körding, K. P. (2008a). Inferring functional connections between neurons. *Current opinion in neurobiology*, 18(6):582–588.

[Stevenson et al., 2008b] Stevenson, I. H., Rebesco, J. M., Miller, L. E., and Körding, K. P. (2008b). Inferring functional connections between neurons. *Curr. Opin. Neurobiol.*, 18(6):582–588.

[Wald, 1940] Wald, A. (1940). The fitting of straight lines if both variables are subject to error. *The Annals of Mathematical Statistics*, 11(3):284–300.

[Wassermann, 2006] Wassermann, L. (2006). All of nonparametric statistics. *New York*.

[Zemelman et al., 2002] Zemelman, B. V., Lee, G. A., Ng, M., and Miesenböck, G. (2002). Selective photostimulation of genetically charged neurons. *Neuron*, 33(1):15–22.